Optical and Quantum Electronics (2024) 56:484
https://doi.org/10.1007/s11082-023-06107-7

Optical wave propagation phase for mKdV spherical electric flux density in sphere space

Talat Körpinar[1] · Fatih Şevgİn[2] · Zeliha Körpinar[3]

Received: 9 August 2023 / Accepted: 13 December 2023 / Published online: 27 January 2024

Abstract
In this article, we illustrate surface flow *alfa*− microfluidical mKdV spherical electromotive phase in sphere space. Also, we obtain antiferromagnetic axially electrical *alfa*−microfluidical mKdV electric flux path circuit. We have electrical *alfa*−microfluidical geometrical mKdV free surface flow density in sphere space. Finally, we design antiferromagnetic wave propagation for *alfa*− microfluidical geometric mKdV surface flux density.

Keywords Optical frame · Wave propagation · Optical surface flow flux · *alfa*−microfluidical · Electromotive phase

PACS 03.50.De · 04.20.-q · 02.40.-k

1 Introduction

Magnetic flux modeling is an important phase investigation approach that is designing the diversion of electromagnetic manufacturers and numerous applied researchers. Magnetic geometric systems are studied enveloping materials, polymers, liquids, foams, optical suspensions, and electromagnetic flux with microfluidic systems (Whitesides 2006; Leber et al. 2018; Eastman et al. 2001; Choi et al. 1999; Rogers et al. 2010; Ryu 2018; Ghadimi et al. 2011; Sun et al. 2017; Sarkar 2011; Ricca 2005; Fukami et al. 2019; Liu et al. 2020; Körpınar et al. 2021e, f; Ling et al. 2016; Körpınar and Körpınar 2021b, 2022c; Dai et al. 2015; Danesh et al. 2012).

✉ Zeliha Körpinar
zelihakorpinar@gmail.com

Talat Körpinar
talatkorpinar@gmail.com

Fatih Şevgİn
f.sevgin@alparslan.edu.tr

[1] Department of Mathematics, Muş Alparslan University, 49250 Muş, Turkey

[2] Department of Construction Technology, Muş Alparslan University, 49250 Muş, Turkey

[3] Department of Administration, Muş Alparslan University, 49250 Muş, Turkey

The great advancements and constructions in the electromotive of the optical microscales are suitable for flux data analysis with development of advanced phase processing approaches. Some recent optical supplements related to evolution and geometric application of optical flux methods for investigation of spinning electromagnetic machines (Körpınar and Körpınar 2021c, 2022a, b; Körpınar et al. 2020a, 2022a; Daneshmehr and Rajabpoor 2014; Farajpour et al. 2014; Ghayesh and Farokhi 2017; Farokhi and Ghayesh 2015; Ghayesh and Farokhi 2017).

Optical geometric microscales are collected optical waves that effect at fixed velocity externally developing geometric shapes. Also, electromagnetic microscales are constructed by an optical phase of nonlinear heat and dynamical influences in complex medium. They are inspected in many optical models for nonlinear heat dynamics with diverse geometric phases of optical wave designs, such as dark, envelope, periodic, bright, compact on, singular, Jacobi elliptic function, optical, and many dynamical forms. Optical technological advancements engage numerical modeling to attend to the optical applications of electromagnetic fields and complex random systems with thermal energy minimizations (Körpınar and Körpınar 2021d, e; Sordo 2019; Körpınar et al. 2020b, 2021a, b, c, 2022b; Yan et al. 2019; Chou and Qu 2001; Marí Beffa et al. 2002; Marí Beffa 2009; Calini and Ivey 2005; Marí Beffa and Olver 2010; Körpınar 2020; Bhatnagar et al. (2019)).

Beneficial to optical soliton solutions to nonlinear heat evolution systems, there are indefinite dynamic modified methods have been established. Dynamical electromagnetic microscale systems are powerful designs for the optical geometric phase of hybrid fibers and spherical electromagnetic flux applications (Korpinar and Körpınar 2021a; Ashkin et al. 1986; Dholakia and Zemánek 2010; Burns et al. 1989; Chaumet and Nieto-Vesperinas 2001; Almaas and Brevik 2013; Körpınar et al. 2019a, b, 2021b; Dholakia and Zemánek 2010; Bliokh 2009; Bliokh et al. 2008; Fukumoto and Miyazaki 1991).

This work is prepared as: In Sect. 2, principle classifications and concepts of mKdV model are given. In Sects. 3–5, we obtain optical wave propagation *alfa*−microfluidic geometrical mKdV electrical flux. Then, we get antiferromagnetic electrical *alfa*−microfluidic geometrical mKdV spherical electromotive phase. Finally, we have axially electrical *alfa*−microfluidic mKdV electric flux path circuit and antiferromagnetic optical *alfa*−microfluidic mKdV electric flux. The conclusion is presented in Sect. 4.

2 Optical *alfa*−mKdV model

Optical mKdV modeling on $\mathbb{S}^2$ is given

$$\mathbf{r}_{\pi} = \mathbf{r}_{sss} + \frac{3}{2}(\mathbf{r}_{ss} \times (\mathbf{r}_{s} \times \mathbf{r}_{ss})) = \frac{1}{2}(1 + \Upsilon^2)\mathbf{t} + \Upsilon_s\mathbf{n},$$

where

$$\begin{aligned}
\mathbf{r}_{\pi} &= \frac{1}{2}(\mathcal{F})\mathbf{t} + \Upsilon_s\mathbf{n}, \\
\mathbf{t}_{\pi} &= -\frac{1}{2}(\mathcal{F})\mathbf{r} + (\frac{1}{2}\Upsilon(\mathcal{F}) + \Upsilon_{ss})\mathbf{n}, \\
\mathbf{n}_{\pi} &= -\Upsilon_s\mathbf{r} - (\Upsilon_{ss} + \frac{1}{2}(\mathcal{F})\Upsilon)\mathbf{t},
\end{aligned}$$

and frame equations are

$$
\begin{aligned}
\mathbf{r}_s =& \mathbf{t}, \\
\mathbf{t}_s =& -\mathbf{r} + \Upsilon \mathbf{n}, \\
\mathbf{n}_s =& -\Upsilon \mathbf{t}.
\end{aligned}
$$

Geometric product is defined

$$\mathbf{t} = \mathbf{n} \times \mathbf{r},\ \mathbf{n} = \mathbf{r} \times \mathbf{t},\ \mathbf{r} = \mathbf{t} \times \mathbf{n}.$$

Compatibility conditons of $\mathbf{t}_{s\pi} = \mathbf{t}_{\pi s},\ \mathbf{n}_{s\pi} = \mathbf{n}_{\pi s}$ is constructred

$$\Upsilon_\pi = \frac{3}{2}\mathcal{F}\Upsilon_s + \Upsilon_{sss},$$

where $\Upsilon^2 + 1 = \mathcal{F}$.

By Lorentz forces we get

$$
\begin{aligned}
\phi(\mathbf{r}) =& \mathbf{t}, \\
\phi(\mathbf{t}) =& -\mathbf{r} + \omega \mathbf{n}, \\
\phi(\mathbf{n}) =& -\omega \mathbf{t}, \\
\mathcal{B}\Im \qquad\qquad & \qquad\qquad \omega \mathbf{r} + \mathbf{n}, \\
\mathcal{E} =& -(\frac{\varpi}{\vartheta} + 1)\mathbf{r} + (\frac{\varpi}{\vartheta}\varkappa + \omega)\mathbf{n}.
\end{aligned}
$$

where $\omega = g(\phi(\mathbf{t}), \mathbf{n})$. Then

$$
\begin{aligned}
\nabla_s \phi(\mathbf{r}) =& -\mathbf{r} + \Upsilon \mathbf{n}, \\
\nabla_s \phi(\mathbf{t}) =& -(1 + \omega\Upsilon)\mathbf{t} + \omega_s \mathbf{n}, \\
\nabla_s \phi(\mathbf{n}) =& \omega \mathbf{r} - \omega_s \mathbf{t} - \omega\Upsilon \mathbf{n}, \\
\nabla_s \mathcal{B}\Im \qquad\qquad & \qquad\qquad \omega_s \mathbf{r} + (\omega - \Upsilon)\mathbf{t}, \\
\nabla_s \mathcal{E} =& -(\frac{\varpi}{\vartheta} + 1)\mathbf{t} + (\omega_s + \frac{\varpi}{\vartheta}\varkappa_s)\mathbf{n} - \Upsilon(\omega + \frac{\varpi}{\vartheta}\varkappa)\mathbf{t},
\end{aligned}
$$

and

$$
\begin{aligned}
\nabla_\pi \mathbf{r} =& \frac{1}{2}(\mathcal{F})\mathbf{t} + \Upsilon_s \mathbf{n}, \\
\nabla_\pi \mathbf{t} =& -\frac{1}{2}(\mathcal{F})\mathbf{r} + (\frac{\Upsilon}{2}(\mathcal{F}) + \Upsilon_{ss})\mathbf{n}, \\
\nabla_\pi \mathbf{n} =& -\Upsilon_s \mathbf{r} - (\Upsilon_{ss} + \frac{\Upsilon}{2}(\mathcal{F}))\mathbf{t}.
\end{aligned}
$$

Also, mKdV motion conditions of fields are

$$
\begin{aligned}
\phi(\mathbf{r}) \times \nabla_s \phi(\mathbf{r}) =& \Upsilon \mathbf{r} + \mathbf{n}, \\
\phi(\mathbf{t}) \times \nabla_s \phi(\mathbf{t}) =& \omega(1 + \omega\Upsilon)\mathbf{r} + \omega_s \mathbf{t} + (1 + \omega\Upsilon)\mathbf{n}, \\
\phi(\mathbf{n}) \times \nabla_s \phi(\mathbf{n}) =& \omega^2 \Upsilon \mathbf{r} + \omega^2 \mathbf{n},
\end{aligned}
$$

and

$$\nabla_\pi \phi(\mathbf{r}) = -\frac{1}{2}(\mathcal{F})\mathbf{r} + (\frac{1}{2}\Upsilon(\mathcal{F}) + \Upsilon_{ss})\mathbf{n},$$
$$\nabla_\pi \phi(\mathbf{t}) = -\Upsilon_s \omega\,\mathbf{r} - (\omega(\Upsilon_{ss} + \frac{\Upsilon}{2}(\mathcal{F})) + \frac{1}{2}(\mathcal{F}))\mathbf{t} + (\omega_\pi - \Upsilon_s)\mathbf{n},$$
$$\nabla_\pi \phi(\mathbf{n}) = \frac{\omega}{2}(\mathcal{F})\mathbf{r} - \omega_\pi \mathbf{t} - \omega(\frac{\Upsilon}{2}(\mathcal{F}) + \Upsilon_{ss})\mathbf{n},$$
$$\nabla_\pi \mathcal{B} = (\omega_\pi - \Upsilon_s)\mathbf{r} + (\frac{\omega}{2}(\mathcal{F}) - (\Upsilon_{ss} + \frac{\Upsilon}{2}(\mathcal{F})))\mathbf{t} + \Upsilon_s \omega \mathbf{n},$$
$$\nabla_\pi \mathcal{E} = -\Upsilon_s(\omega + \frac{\varpi}{\vartheta}\varkappa)\mathbf{r} - (\frac{1}{2}(\frac{\varpi}{\vartheta} + 1)(\mathcal{F}) + (\Upsilon_{ss} + \frac{\Upsilon}{2}(\mathcal{F}))(\omega + \frac{\varpi}{\vartheta}\varkappa))\mathbf{t}$$
$$+ ((\omega_\pi + \frac{\varpi}{\vartheta}\varkappa_\pi) - \Upsilon_s(\frac{\varpi}{\vartheta} + 1))\mathbf{n}.$$

3 Wave propagation for *alfa*−microfluidical geometric mKdV electric $\phi(\mathbf{r})$ flux

Surface flow alfa− microfluidical geometric mKdV spherical electromotive $\phi(\mathbf{r})$ phase is

$$\boldsymbol{E}^{\mathcal{E}}\phi(\boldsymbol{\alpha}) = -\frac{d}{d\pi}\int_{\mathcal{F}} (-(\frac{1}{2}(\frac{\varpi}{\vartheta} + 1)(\mathcal{F}) + (\Upsilon_{ss} + \frac{\Upsilon}{2}(\mathcal{F}))(\omega + \frac{\varpi}{\vartheta}\varkappa))(\frac{1}{2}\Upsilon(\mathcal{F}) + \Upsilon_{ss} - \frac{1}{2}(\mathcal{F})\Upsilon))d\mathcal{F}.$$

In a similar product, we get

$$\nabla_s \phi(\mathbf{r}) \times \nabla_\pi \phi(\mathbf{r}) = (\frac{1}{2}\Upsilon(\mathcal{F}) + \Upsilon_{ss} - \frac{1}{2}(\mathcal{F})\Upsilon)\mathbf{t}.$$

Electrical alfa−microfluidical optical geometric mKdV free $\phi(\mathbf{r})$ surface flow density is

$$\boldsymbol{L}^{\mathcal{E}}\phi(\mathbf{r}) \Im -(\frac{1}{2}(\frac{\varpi}{\vartheta} + 1)(\mathcal{F}) + (\Upsilon_{ss} + \frac{\Upsilon}{2}(\mathcal{F}))(\omega + \frac{\varpi}{\vartheta}\varkappa))(\frac{1}{2}\Upsilon(\mathcal{F}) + \Upsilon_{ss} - \frac{1}{2}(\mathcal{F})\Upsilon).$$

Wave propagation for alfa− microfluidical geometric mKdV electric $\phi(\mathbf{r})$ flux is

$$\boldsymbol{W}^{\mathcal{E}}\phi(\mathbf{r}) = \int_{\mathcal{F}} (-(\frac{1}{2}(\frac{\varpi}{\vartheta} + 1)(\mathcal{F}) + (\Upsilon_{ss} + \frac{\Upsilon}{2}(\mathcal{F}))(\omega + \frac{\varpi}{\vartheta}\varkappa))(\frac{1}{2}\Upsilon(\mathcal{F}) + \Upsilon_{ss} - \frac{1}{2}(\mathcal{F})\Upsilon))d\mathcal{F}.$$

Also, we get

$$\nabla_s \phi(\mathbf{r}) \times \phi(\mathbf{r}) \times \nabla_s \phi(\mathbf{r}) = -(\mathcal{F})\mathbf{t}.$$

Antiferromagnetic electrical alfa− microfluidical axially mKdV free $\phi(\mathbf{r})$ surface flow density is

$$^{\mathcal{AF}}\boldsymbol{L}^{\mathcal{E}}\phi(\mathbf{r}) = (\mathcal{F})(\frac{1}{2}(\frac{\varpi}{\vartheta} + 1)(\mathcal{F}) + (\Upsilon_{ss} + \frac{\Upsilon}{2}(\mathcal{F}))(\omega + \frac{\varpi}{\vartheta}\varkappa)).$$

Antiferromagnetic wave propagation for alfa–microfluidical geometric mKdV electric $\phi(\mathbf{r})$ flux is

$$^{\mathcal{AF}}\mathbf{W}^{\mathcal{E}}\phi(\mathbf{r}) = \int_{\mathcal{F}} ((\mathcal{F})(\frac{1}{2}(\frac{\varpi}{\vartheta}+1)(\mathcal{F}) + (\Upsilon_{ss} + \frac{\Upsilon}{2}(\mathcal{F}))(\omega + \frac{\varpi}{\vartheta}\varkappa)))d\mathcal{F}.$$

Axially electrical alfa– microfluidical mKdV electric $\phi(\mathbf{r})$ flux path circuit is

$$-(\frac{1}{2}(\frac{\varpi}{\vartheta}+1)(\mathcal{F}) + (\Upsilon_{ss} + \frac{\Upsilon}{2}(\mathcal{F}))(\omega + \frac{\varpi}{\vartheta}\varkappa))(\frac{1}{2}\Upsilon(\mathcal{F}) + \Upsilon_{ss} - \frac{1}{2}(\mathcal{F})\Upsilon) = 0.$$

Antiferromagnetic axially electrical alfa–microfluidical mKdV electric $\phi(\mathbf{r})$ flux path circuit is

$$(\mathcal{F})(\frac{1}{2}(\frac{\varpi}{\vartheta}+1)(\mathcal{F}) + (\Upsilon_{ss} + \frac{\Upsilon}{2}(\mathcal{F}))(\omega + \frac{\varpi}{\vartheta}\varkappa)) = 0.$$

Antiferromagnetic surface flow alfa– microfluidical mKdV spherical electromotive $\phi(\mathbf{r})$ phase is

$$^{\mathcal{AF}}\boldsymbol{E}^{\mathcal{E}}\phi(\mathbf{r}) = -\frac{d}{d\pi}\int_{\mathcal{F}} ((\mathcal{F})(\frac{1}{2}(\frac{\varpi}{\vartheta}+1)(\mathcal{F}) + (\Upsilon_{ss} + \frac{\Upsilon}{2}(\mathcal{F}))(\omega + \frac{\varpi}{\vartheta}\varkappa)))d\mathcal{F}.$$

Figure 1 illustrates optical effect of diverse values of the thermal diffusion amplitude on axially antiferromagnetic wave propagation for *alfa*–microfluidical geometric mKdV electric $\phi(\mathbf{r})$ flux path circuit of geometric system.

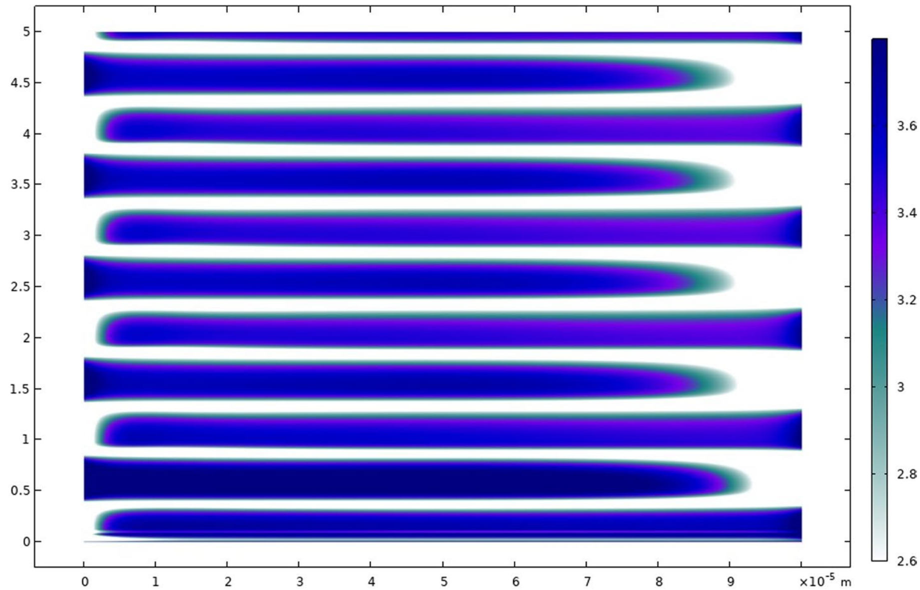

Fig. 1 Wave propagation for *alfa*–microfluidical geometric mKdV electric $\phi(\mathbf{r})$ flux

4 Wave propagation for *alfa*–microfluidical geometric mKdV electric $\boldsymbol{\phi}(\mathbf{t})$ flux

Surface flow alfa– microfluidical geometric mKdV spherical electromotive $\phi(\mathbf{t})$ phase is

$$
\begin{aligned}
\boldsymbol{E}^{\mathcal{E}}\phi(\mathbf{t}) = -\frac{d}{d\pi}\int_{\mathcal{F}}&(-\Upsilon_s(\omega+\frac{\varpi}{\vartheta}\varkappa)(\omega_s(\omega(\Upsilon_{ss}+\frac{\Upsilon}{2}(\mathcal{F}))\\
&+\frac{1}{2}(\mathcal{F}))-(1+\omega\Upsilon)(\omega_\pi-\Upsilon_s))+\Upsilon_s^2(\frac{\varpi}{\vartheta}+1))(1+\omega\Upsilon)\omega\\
&+\Upsilon_s\omega\omega_s(\frac{1}{2}(\frac{\varpi}{\vartheta}+1)(\mathcal{F})+(\Upsilon_{ss}+\frac{\Upsilon}{2}(\mathcal{F}))(\omega+\frac{\varpi}{\vartheta}\varkappa)))d\mathcal{F}.
\end{aligned}
$$

By utilizing product

$$
\begin{aligned}
\nabla_s\phi(\mathbf{t})\times\nabla_\pi\phi(\mathbf{t}) = (\omega_s(\omega(\Upsilon_{ss}+\frac{\Upsilon}{2}(\mathcal{F}))+\frac{1}{2}(\mathcal{F}))\\
-(1+\omega\Upsilon)(\omega_\pi-\Upsilon_s))\mathbf{r}-\Upsilon_s\omega\omega_s\mathbf{t}-(1+\omega\Upsilon)\Upsilon_s\omega\mathbf{n}.
\end{aligned}
$$

Electrical alfa–microfluidical optical geometric mKdV free $\phi(\mathbf{t})$ surface flow density is

$$
\begin{aligned}
\boldsymbol{L}^{\mathcal{E}}\phi(\mathbf{t}) = &-\Upsilon_s(\omega+\frac{\varpi}{\vartheta}\varkappa)(\omega_s(\omega(\Upsilon_{ss}+\frac{\Upsilon}{2}(\mathcal{F}))+\frac{1}{2}(\mathcal{F}))\\
&-(1+\omega\Upsilon)(\omega_\pi-\Upsilon_s))+\Upsilon_s\omega\omega_s(\frac{1}{2}(\frac{\varpi}{\vartheta}+1)(\mathcal{F})+(\Upsilon_{ss}\\
&+\frac{\Upsilon}{2}(\mathcal{F}))(\omega+\frac{\varpi}{\vartheta}\varkappa))+\Upsilon_s^2(\frac{\varpi}{\vartheta}+1))(1+\omega\Upsilon)\omega.
\end{aligned}
$$

Wave propagation for alfa– microfluidical geometric mKdV electric $\phi(\mathbf{t})$ flux is

$$
\begin{aligned}
\boldsymbol{W}^{\mathcal{E}}\phi(\mathbf{t}) = \int_{\mathcal{F}}&(\Upsilon_s\omega\omega_s(\frac{1}{2}(\frac{\varpi}{\vartheta}+1)(\mathcal{F})+(\Upsilon_{ss}+\frac{\Upsilon}{2}(\mathcal{F}))(\omega\\
&+\frac{\varpi}{\vartheta}\varkappa))+\Upsilon_s^2(\frac{\varpi}{\vartheta}+1))(1+\omega\Upsilon)\omega-\Upsilon_s(\omega+\frac{\varpi}{\vartheta}\varkappa)(\omega_s(\omega(\Upsilon_{ss}\\
&+\frac{\Upsilon}{2}(\mathcal{F}))+\frac{1}{2}(\mathcal{F}))-(1+\omega\Upsilon)(\omega_\pi-\Upsilon_s)))d\mathcal{F}.
\end{aligned}
$$

On the other hand, we have

$$
\begin{aligned}
\nabla_s\phi(\mathbf{t}) &= -(1+\omega\Upsilon)\mathbf{t}+\omega_s\mathbf{n},\\
\phi(\mathbf{t})\times\nabla_s\phi(\mathbf{t}) &= \omega(1+\omega\Upsilon)\mathbf{r}+\omega_s\mathbf{t}+(1+\omega\Upsilon)\mathbf{n},\\
\nabla_s\phi(\mathbf{t})\times\phi(\mathbf{t})\times\nabla_s\phi(\mathbf{t}) &= -(\omega_s^2+(1+\omega\Upsilon)^2)\mathbf{r}+\omega_s\omega(1+\omega\Upsilon)\mathbf{t}+\omega(1+\omega\Upsilon)^2\mathbf{n}.
\end{aligned}
$$

Antiferromagnetic electrical alfa– microfluidical axially mKdV free $\phi(\mathbf{t})$ surface flow density is

$$
\begin{aligned}
{}^{\mathcal{AF}}\boldsymbol{L}^{\mathcal{E}}\phi(\mathbf{t}) = &\Upsilon_s(\omega+\frac{\varpi}{\vartheta}\varkappa)(\omega_s^2+(1+\omega\Upsilon)^2)-\omega_s(\frac{1}{2}(\frac{\varpi}{\vartheta}\\
&+1)(\mathcal{F})+(\Upsilon_{ss}+\frac{\Upsilon}{2}(\mathcal{F}))(\omega+\frac{\varpi}{\vartheta}\varkappa))\omega(1+\omega\Upsilon)\\
&+\omega(1+\omega\Upsilon)^2((\omega_\pi+\frac{\varpi}{\vartheta}\varkappa_\pi)-\Upsilon_s(\frac{\varpi}{\vartheta}+1)).
\end{aligned}
$$

Antiferromagnetic wave propagation for alfa–microfluidical geometric mKdV electric $\phi(\mathbf{t})$ flux is

$$
\begin{aligned}
{}^{\mathcal{AF}}\mathbf{W}^{\mathcal{E}}\phi(\mathbf{t}) = \int_{\mathcal{F}} & (\omega(1+\omega\Upsilon)^2((\omega_\pi + \frac{\varpi}{\vartheta}\varkappa_\pi) - \Upsilon_s(\frac{\varpi}{\vartheta}+1)) \\
& + \Upsilon_s(\omega + \frac{\varpi}{\vartheta}\varkappa)(\omega_s^2 + (1+\omega\Upsilon)^2) - \omega_s(\frac{1}{2}(\frac{\varpi}{\vartheta}+1)(\mathcal{F}) \\
& + (\Upsilon_{ss} + \frac{\Upsilon}{2}(\mathcal{F}))(\omega + \frac{\varpi}{\vartheta}\varkappa))\omega(1+\omega\Upsilon))d\mathcal{F}.
\end{aligned}
$$

Axially electrical alfa– microfluidical geometric mKdV electric $\phi(\mathbf{t})$ flux path circuit is

$$
\begin{aligned}
& \Upsilon_s^2(\frac{\varpi}{\vartheta}+1))(1+\omega\Upsilon)\omega - \Upsilon_s(\omega + \frac{\varpi}{\vartheta}\varkappa)(\omega_s(\omega(\Upsilon_{ss} + \frac{\Upsilon}{2}(\mathcal{F})) \\
& + \frac{1}{2}(\mathcal{F})) - (1+\omega\Upsilon)(\omega_\pi - \Upsilon_s)) + \Upsilon_s\omega\omega_s(\frac{1}{2}(\frac{\varpi}{\vartheta} \\
& + 1)(\mathcal{F}) + (\Upsilon_{ss} + \frac{\Upsilon}{2}(\mathcal{F}))(\omega + \frac{\varpi}{\vartheta}\varkappa)) = 0.
\end{aligned}
$$

Antiferromagnetic axially electrical alfa–microfluidical mKdV electric $\phi(\mathbf{t})$ flux path circuit is

$$
\begin{aligned}
& \omega(1+\omega\Upsilon)^2((\omega_\pi + \frac{\varpi}{\vartheta}\varkappa_\pi) - \Upsilon_s(\frac{\varpi}{\vartheta}+1)) - \omega_s(\frac{1}{2}(\frac{\varpi}{\vartheta} \\
& + 1)(\mathcal{F}) + (\Upsilon_{ss} + \frac{\Upsilon}{2}(\mathcal{F}))(\omega + \frac{\varpi}{\vartheta}\varkappa))\omega(1+\omega\Upsilon) \\
& + \Upsilon_s(\omega + \frac{\varpi}{\vartheta}\varkappa)(\omega_s^2 + (1+\omega\Upsilon)^2) = 0.
\end{aligned}
$$

Antiferromagnetic surface flow alfa– microfluidical mKdV spherical electromotive $\phi(\mathbf{t})$ phase is

$$
\begin{aligned}
{}^{\mathcal{AF}}\boldsymbol{E}^{\mathcal{E}}\phi(\mathbf{t}) = -\frac{d}{d\pi}\int_{\mathcal{F}} & (-\omega_s(\frac{1}{2}(\frac{\varpi}{\vartheta}+1)(\mathcal{F}) + (\Upsilon_{ss} \\
& + \frac{\Upsilon}{2}(\mathcal{F}))(\omega + \frac{\varpi}{\vartheta}\varkappa))\omega(1+\omega\Upsilon) + \Upsilon_s(\omega + \frac{\varpi}{\vartheta}\varkappa)(\omega_s^2 \\
& + (1+\omega\Upsilon)^2) + \omega(1+\omega\Upsilon)^2((\omega_\pi + \frac{\varpi}{\vartheta}\varkappa_\pi) - \Upsilon_s(\frac{\varpi}{\vartheta}+1)))d\mathcal{F}.
\end{aligned}
$$

Figure 2 illustrates optical effect of diverse values of the thermal diffusion amplitude on axially antiferromagnetic wave propagation for *alfa*–microfluidical geometric mKdV electric $\phi(\mathbf{t})$ flux path circuit of geometric system.

5 Wave propagation for *alfa*–microfluidical geometric mKdV electric $\boldsymbol{\phi}(\mathbf{n})$ flux

Surface flow alfa– microfluidical geometric mKdV spherical electromotive $\phi(\mathbf{n})$ phase is

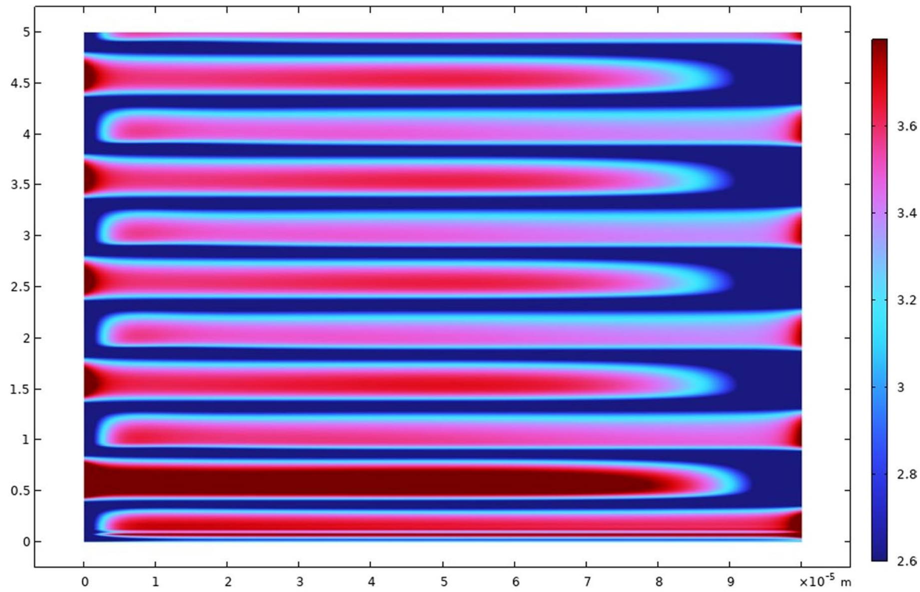

Fig. 2 Wave propagation for *alfa*− microfluidical geometric mKdV electric $\phi(\mathbf{r})$ flux

$$\begin{aligned}\boldsymbol{E}^{\mathcal{E}}\phi(\mathbf{n}) = & -\frac{d}{d\pi}\int_{\mathcal{F}}(-(\omega^2(\frac{\Upsilon}{2}(\mathcal{F})+\Upsilon_{ss})-\frac{\Upsilon\omega^2}{2}(\Upsilon^2\\ & +1))(\frac{1}{2}(\frac{\varpi}{\vartheta}+1)(\mathcal{F})+(\Upsilon_{ss}+\frac{\Upsilon}{2}(\mathcal{F}))(\omega+\frac{\varpi}{\vartheta}\varkappa))\\ & +(\frac{\omega\omega_s}{2}(\mathcal{F})-\omega_\pi\omega)((\omega_\pi+\frac{\varpi}{\vartheta}\varkappa_\pi)-\Upsilon_s(\frac{\varpi}{\vartheta}+1))\\ & -\Upsilon_s(\omega+\frac{\varpi}{\vartheta}\varkappa)(\omega_s\omega(\frac{\Upsilon}{2}(\mathcal{F})+\Upsilon_{ss})-\omega\Upsilon\omega_\pi))d\mathcal{F}.\end{aligned}$$

So, cross product is computed as follows

$$\begin{aligned}\nabla_s\phi(\mathbf{n}) =& \omega\mathbf{r}-\omega_s\mathbf{t}-\omega\Upsilon\mathbf{n},\\ \nabla_\pi\phi(\mathbf{n}) =& \frac{\omega}{2}(\mathcal{F})\mathbf{r}-\omega_\pi\mathbf{t}-\omega(\frac{\Upsilon}{2}(\mathcal{F})+\Upsilon_{ss})\mathbf{n},\\ \nabla_s\phi(\mathbf{n})\times\nabla_\pi\phi(\mathbf{n}) =& (\omega_s\omega(\frac{\Upsilon}{2}(\mathcal{F})+\Upsilon_{ss})-\omega\Upsilon\omega_\pi)\mathbf{r}\\ & +(\omega^2(\frac{\Upsilon}{2}(\mathcal{F})+\Upsilon_{ss})-\frac{\Upsilon\omega^2}{2}(\mathcal{F}))\mathbf{t}+(\frac{\omega\omega_s}{2}(\mathcal{F})-\omega_\pi\omega)\mathbf{n}.\end{aligned}$$

Electrical alfa–microfluidical optical geometric mKdV free $\phi(\mathbf{n})$ *surface flow density is*

$$\begin{aligned}\boldsymbol{L}^{\mathcal{E}}\phi(\mathbf{n}) = & -\Upsilon_s(\omega+\frac{\varpi}{\vartheta}\varkappa)(\omega_s\omega(\frac{\Upsilon}{2}(\mathcal{F})+\Upsilon_{ss})-\omega\Upsilon\omega_\pi)-(\omega^2(\frac{\Upsilon}{2}(\mathcal{F})\\ & +\Upsilon_{ss})-\frac{\Upsilon\omega^2}{2}(\mathcal{F}))(\frac{1}{2}(\frac{\varpi}{\vartheta}+1)(\mathcal{F})+(\Upsilon_{ss}+\frac{\Upsilon}{2}(\mathcal{F}))(\omega\\ & +\frac{\varpi}{\vartheta}\varkappa))+(\frac{\omega\omega_s}{2}(\mathcal{F})-\omega_\pi\omega)((\omega_\pi+\frac{\varpi}{\vartheta}\varkappa_\pi)-\Upsilon_s(\frac{\varpi}{\vartheta}+1))\end{aligned}$$

Wave propagation for alfa− microfluidical geometric mKdV electric $\phi(\mathbf{n})$ flux is

$$\begin{aligned}\boldsymbol{W}^{\mathcal{E}}\phi(\mathbf{n}) = \int_{\mathcal{F}} &((\frac{\omega\omega_s}{2}(\mathcal{F}) - \omega_\pi\omega)((\omega_\pi + \frac{\varpi}{\vartheta}\varkappa_\pi) - \Upsilon_s(\frac{\varpi}{\vartheta} + 1))\\ &- \Upsilon_s(\omega + \frac{\varpi}{\vartheta}\varkappa)(\omega_s\omega(\frac{\Upsilon}{2}(\mathcal{F}) + \Upsilon_{ss}) - \omega\Upsilon\omega_\pi) - (\omega^2(\frac{\Upsilon}{2}(\mathcal{F}) + \Upsilon_{ss})\\ &- \frac{\Upsilon\omega^2}{2}(\mathcal{F}))(\frac{1}{2}(\frac{\varpi}{\vartheta} + 1)(\mathcal{F}) + (\Upsilon_{ss} + \frac{\Upsilon}{2}(\mathcal{F}))(\omega + \frac{\varpi}{\vartheta}\varkappa)))d\mathcal{F}.\end{aligned}$$

Since

$$\begin{aligned}\nabla_s\phi(\mathbf{n}) &= \omega\mathbf{r} - \omega_s\mathbf{t} - \omega\Upsilon\mathbf{n}\\ \phi(\mathbf{n}) \times \nabla_s\phi(\mathbf{n}) &= \omega^2\Upsilon\mathbf{r} + \omega^2\mathbf{n}\\ \nabla_s\phi(\mathbf{n}) \times \phi(\mathbf{n}) \times \nabla_s\phi(\mathbf{n}) &= -\omega_s\omega^2\mathbf{r} - (\omega^3 + \omega^3\Upsilon^2)\mathbf{t} + \omega^2\Upsilon\omega_s\mathbf{n}\end{aligned}$$

Antiferromagnetic electrical alfa− microfluidical axially mKdV free $\phi(\mathbf{n})$ surface flow density is

$$\begin{aligned}{}^{\mathcal{AF}}\boldsymbol{L}^{\mathcal{E}}\phi(\mathbf{n}) = &\omega_s\omega^2\Upsilon_s(\omega + \frac{\varpi}{\vartheta}\varkappa) + (\frac{1}{2}(\frac{\varpi}{\vartheta} + 1)(\mathcal{F})\\ &+ (\Upsilon_{ss} + \frac{\Upsilon}{2}(\mathcal{F}))(\omega + \frac{\varpi}{\vartheta}\varkappa))(\omega^3 + \omega^3\Upsilon^2)\\ &+ \omega^2\Upsilon\omega_s((\omega_\pi + \frac{\varpi}{\vartheta}\varkappa_\pi) - \Upsilon_s(\frac{\varpi}{\vartheta} + 1))\end{aligned}$$

Antiferromagnetic wave propagation for alfa−microfluidical geometric mKdV electric $\phi(\mathbf{n})$ flux is

$$\begin{aligned}{}^{\mathcal{AF}}\mathbf{W}^{\mathcal{E}}\phi(\mathbf{n}) = \int_{\mathcal{F}} &(((\omega_\pi + \frac{\varpi}{\vartheta}\varkappa_\pi) - \Upsilon_s(\frac{\varpi}{\vartheta} + 1))\omega^2\Upsilon\omega_s\\ &+ \omega_s\omega^2\Upsilon_s(\omega + \frac{\varpi}{\vartheta}\varkappa) + (\frac{1}{2}(\frac{\varpi}{\vartheta} + 1)(\mathcal{F})\\ &+ (\Upsilon_{ss} + \frac{\Upsilon}{2}(\mathcal{F}))(\omega + \frac{\varpi}{\vartheta}\varkappa))(\omega^3 + \omega^3\Upsilon^2))d\mathcal{F}.\end{aligned}$$

Axially electrical alfa− microfluidical geometric mKdV electric $\phi(\mathbf{n})$ flux path circuit is

$$\begin{aligned}&-(\omega^2(\frac{\Upsilon}{2}(\mathcal{F}) + \Upsilon_{ss}) - \frac{\Upsilon\omega^2}{2}(\mathcal{F}))(\frac{1}{2}(\frac{\varpi}{\vartheta} + 1)(\mathcal{F})\\ &+ (\Upsilon_{ss} + \frac{\Upsilon}{2}(\mathcal{F}))(\omega + \frac{\varpi}{\vartheta}\varkappa)) - \Upsilon_s(\omega + \frac{\varpi}{\vartheta}\varkappa)(\omega_s\omega(\frac{\Upsilon}{2}(\mathcal{F}) + \Upsilon_{ss})\\ &- \omega\Upsilon\omega_\pi) + (\frac{\omega\omega_s}{2}(\mathcal{F}) - \omega_\pi\omega)((\omega_\pi + \frac{\varpi}{\vartheta}\varkappa_\pi) - \Upsilon_s(\frac{\varpi}{\vartheta} + 1)) = 0.\end{aligned}$$

Antiferromagnetic axially electrical alfa−microfluidical mKdV electric $\phi(\mathbf{n})$ flux path circuit is

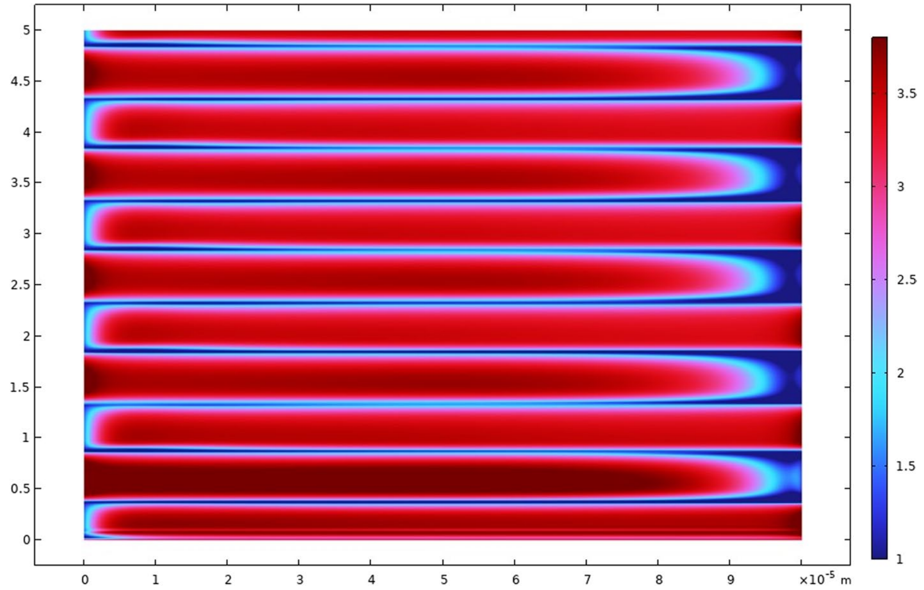

Fig. 3 Wave propagation for *alfa*− microfluidical geometric mKdV electric $\phi(\mathbf{r})$ flux

$$
\begin{aligned}
&\omega_s((\omega_\pi + \frac{\varpi}{\vartheta}\varkappa_\pi) - \Upsilon_s(\frac{\varpi}{\vartheta} + 1))\omega^2\Upsilon \\
&\quad + \omega_s\omega^2\Upsilon_s(\omega + \frac{\varpi}{\vartheta}\varkappa) + (\frac{1}{2}(\frac{\varpi}{\vartheta} + 1)(\mathcal{F}) \\
&\quad + (\Upsilon_{ss} + \frac{\Upsilon}{2}(\mathcal{F}))(\omega + \frac{\varpi}{\vartheta}\varkappa))(\omega^3 + \omega^3\Upsilon^2) = 0.
\end{aligned}
$$

Antiferromagnetic surface flow alfa− microfluidical mKdV spherical electromotive $\phi(\mathbf{n})$ *phase is*

$$
\begin{aligned}
{}^{\mathcal{AF}}\boldsymbol{E}^{\mathcal{E}}\phi(\mathbf{n}) = &-\frac{d}{d\pi}\int_{\mathcal{F}}((\frac{1}{2}(\frac{\varpi}{\vartheta} + 1)(\mathcal{F}) + (\Upsilon_{ss} \\
&+ \frac{\Upsilon}{2}(\mathcal{F}))(\omega + \frac{\varpi}{\vartheta}\varkappa))(\omega^3 + \omega^3\Upsilon^2) + \omega^2\Upsilon\omega_s((\omega_\pi \\
&+ \frac{\varpi}{\vartheta}\varkappa_\pi) - \Upsilon_s(\frac{\varpi}{\vartheta} + 1)) + \Upsilon_s(\omega + \frac{\varpi}{\vartheta}\varkappa)\omega_s\omega^2)d\mathcal{F}.
\end{aligned}
$$

Figure 3 illustrates optical effect of diverse values of the thermal diffusion amplitude on axially antiferromagnetic wave propagation for *alfa*−microfluidical geometric mKdV electric $\phi(\mathbf{n})$ flux path circuit of geometric system.

6 Conclusion

The optical geometric model for antiferromagnetic wave propagation *alfa*− microfluidical mKdV spherical electromotive phase is constructed for the first time in this study. Also, we obtain antiferromagnetic axially electrical *alfa*−microfluidical mKdV electric flux path circuit. We have electrical *alfa*−microfluidical geometrical mKdV free surface flow density in sphere space. Finally, we design antiferromagnetic wave propagation for *alfa*−microfluidical geometric mKdV surface flux density.

Author contributions All authors of this research paper have directly participated in the planning, execution, or analysis of this study; All authors of this paper have read and approved the final version submitted.

Funding Open access funding provided by the Scientific and Technological Research Council of Türkiye (TÜBİTAK). No funding was received for the study.

Declarations

Ethical approval The contents of this manuscript have not been copyrighted or published previously; The contents of this manuscript are not now under consideration for publication elsewhere.

Conflict of interest The authors declare that they have no known competing financial interests or personal relationships that could have appeared to influence the work reported in this paper.

Availability of data and materials No data was used for the research described in the article.

References

Almaas, E., Brevik, I.: Possible sorting mechanism for microparticles in an evanescent field. Phys. Rev. A **87**, 063826 (2013)

Ashkin, A., Dziedzic, J.M., Bjorkholm, J.E., Chu, S.: Observation of a single-beam gradient force optical trap for dielectric particles. Opt. Lett. **11**, 288–290 (1986)

Bhatnagar, S., Afshar, Y., Pan, S., Duraisamy, K., Kaushik, S.: Prediction of aerodynamic flow fields using convolutional neural networks. Comput. Mech. **64**(2), 525–545 (2019)

Bliokh, K.Y.: Geometrodynamics of polarized light: Berry phase and spin Hall effect in a gradient-index medium. J. Opt. A: Pure Appl. Opt. **11**(9), 094009 (2009)

Bliokh, K.Y., Niv, A., Kleiner, V., Hasman, E.: Geometrodynamics of spinning light. Nat. Photonics **2**(12), 748 (2008)

Burns, M.M., Fournier, J.-M., Golovchenko, J.A.: Optical binding. Phys. Rev. Lett. **63**, 1233–1236 (1989)

Calini, A., Ivey, T.: Finite-gap solutions of the vortex filament equation genus one solutions and symmetric solutions. J. Nonlinear Sci. **15**, 321–361 (2005)

Chaumet, P.C., Nieto-Vesperinas, M.: Optical binding of particles with or without the presence of a flat dielectric surface. Phys. Rev. B **64**, 035422 (2001)

Choi, S.U.S., Li, S., Eastman, J.A.: Measuring thermal conductivity of fluids containing oxide nanoparticles. J. Heat Transf. **121**(2), 280–289 (1999)

Chou, K.S., Qu, C.Z.: The KdV equation and motion of plane curves. J. Phys. Soc. Jan. **70**, 1912–1916 (2001)

Dai, H., Wang, Y., Wang, L.: Nonlinear dynamics of cantilevered microbeams based on modified couple stress theory. Int. J. Eng. Sci. **94**, 103–112 (2015)

Danesh, M., Farajpour, A., Mohammadi, M.: Axial vibration analysis of a tapered nanorod based on nonlocal elasticity theory and differential quadrature method. Mech. Res. Commun. **39**, 23–27 (2012)

Daneshmehr, A., Rajabpoor, A.: Stability of size dependent functionally graded nanoplate based on nonlocal elasticity and higher order plate theories and different boundary conditions. Int. J. Eng. Sci. **82**, 84–100 (2014)

Dholakia, K., Zemánek, P.: Colloquium: gripped by light: optical binding. Rev. Mod. Phys. **82**, 1767–1791 (2010)

Dholakia, K., Zemánek, P.: Colloquium: gripped by light: optical binding. Rev. Mod. Phys. **82**, 1767–1791 (2010)

Eastman, J.A., Choi, S.U.S., Li, S., Yu, W., Thompson, L.J.: Anomalously increased effective thermal conductivities of ethylene glycol-based nanofluids containing copper nanoparticles. Appl. Phys. Lett. **78**(6), 718–720 (2001)

Farajpour, A., Rastgoo, A., Mohammadi, M.: Surface effects on the mechanical characteristics of microtubule networks in living cells. Mech. Res. Commun. **57**, 18–26 (2014)

Farokhi, H., Ghayesh, M.H.: Dynamical behaviour of electrically actuated microcantilevers. Coupled Syst. Mech. **4**, 251–262 (2015)

Fukami, K., Fukagata, K., Taira, K.: Super-resolution reconstruction of turbulent flows with machine learning. J. Fluid Mech. **870**, 106–120 (2019)

Fukumoto, Y., Miyazaki, T.: Three-dimensional distortions of a vortex filament with axial velocity. J. Fluid Mech. **222**, 369–416 (1991)

Ghadimi, A., Saidur, R., Metselaar, H.S.C.: A review of nanofluid stability properties and characterization in stationary conditions. Int. J. Heat Mass Transf. **54**(17–18), 4051–4068 (2011)

Ghayesh, M.H., Farokhi, H.: Nonlinear mechanics of doubly curved shallow microshells. Int. J. Eng. Sci. **119**, 288–304 (2017)

Ghayesh, M.H., Farokhi, H.: Parametric vibrations of imperfect Timoshenko microbeams. Microsyst. Technol. **23**, 4917–4929 (2017)

Körpınar, T.: Optical directional binormal magnetic flows with geometric phase: Heisenberg ferromagnetic model. Optik **219**, 165134 (2020)

Korpinar, T., Körpınar, Z.: Timelike spherical magnetic $\mathbb{S}_{\mathbf{N}}$ flux flows with Heisenberg sphericalferromagnetic spin with some solutions. Optik **242**, 166745 (2021a)

Körpınar, Z., Körpınar, T.: Optical tangent hybrid electromotives for tangent hybrid magnetic particle. Optik **247**, 167823 (2021b)

Körpınar, Z., Körpınar, T.: Optical hybrid electric and magnetic B_1-phase with Landau Lifshitz approach. Optik **247**, 167917 (2021c)

Körpınar, Z., Körpınar, T.: Optical tangent hybrid electromotives for tangent hybrid magnetic particle. Optik **247**, 167823 (2021d)

Körpınar, T., Körpınar, Z.: Spherical electric and magnetic phase with Heisenberg spherical ferromagnetic spin by some fractional solutions. Optik **242**, 167164 (2021e)

Körpınar, Z., Korpinar, T.: Optical spherical electroosmotic phase and optical energy for spherical α-magnetic particles. Optik **255**, 168455 (2022a)

Körpınar, Z., Korpinar, T.: Optical antiferromagnetic electric $\mathbb{S}\alpha$-flux with electroosmotic velocity in Heisenberg $\mathbb{S}^2_{\mathbb{H}}$. Optik **252**, 168206 (2022b)

Körpınar, T., Körpınar, Z.: Optical electromagnetic flux particles with optical antiferromagnetic model. Optik **251**, 168301 (2022c)

Körpınar, T., Demirkol, R.C., Körpınar, Z.: Soliton propagation of electromagnetic field vectors of polarized light ray traveling in a coiled optical fiber in Minkowski space with Bishop equations. Eur. Phys. J. D **73**(9), 203 (2019a)

Körpınar, T., Demirkol, R.C., Körpınar, Z.: Soliton propagation of electromagnetic field vectors of polarized light ray traveling in a coiled optical fiber in the ordinary space. Int. J. Geom. Methods in Modern Phys. **16**(8), 1950117 (2019b)

Körpınar, T., Demirkol, R.C., Körpınar, Z., Asil, V.: Maxwellian evolution equations along the uniform optical fiber in Minkowski space. Revista Mexicana de Física **66**(4), 431–439 (2020a)

Körpınar, T., Körpınar, Z., Demirkol, R.C.: Binormal schrodinger system of wave propagation field of light radiate in the normal direction with q-HATM approach. Optik **235**, 166444 (2020b)

Körpınar, T., Demirkol, R.C., Körpınar, Z.: Optical magnetic helicity with binormal electromagnetic vortex filament flows in MHD. Optik **247**, 167823 (2021a)

Körpınar, T., Demirkol, R.C., Körpınar, Z.: Polarization of propagated light with optical solitons along the fiber in de-sitter space. Optik **226**, 165872 (2021b)
Körpınar, T., Demirkol, R.C., Körpınar, Z.: Approximate solutions for the inextensible Heisenberg antiferromagnetic flow and Solitonic magnetic flux surfaces in the normal direction in Minkowski space. Optik **238**, 166403 (2021c)
Körpınar, T., Demirkol, R.C., Körpınar, Z.: Elastic magnetic curves of ferromagnetic and superparamagnetic models. Math. Methods Appl. Sci. **44**(7), 5797–5820 (2021d)
Körpınar, T., Körpınar, Z., Yeneroğlu, M.: Optical energy of spherical velocity with optical magnetic density in Heisenberg sphere space $\mathbb{S}^2_{Heis^3}$. Optik **247**, 167937 (2021e)
Körpınar, T., Sazak, A., Körpınar, Z.: Optical effects of some motion equations on quasi-frame with compatible Hasimoto map. Optik **247**, 167914 (2021f)
Körpınar, T., Körpınar, Z., Asil, V.: Electric flux particles with spherical antiferromagnetic approach with electroosmotic velocity. Optik **252**, 168108 (2022a)
Körpınar, T., Körpınar, Z., Asil, V.: New approach for optical electroostimistic phase with optical quasi potential energy. Optik **251**, 168291 (2022b)
Leber, A., Cholst, B., Sandt, J., Vogel, N., Kolle, M.: Stretchable thermoplastic elastomer optical fibers for sensing of extreme deformations. Adv. Funct. Mater. **29**, 1802629 (2018)
Ling, J., Kurzawski, A., Templeton, J.: Reynolds averaged turbulence modelling using deep neural networks with embedded invariance. J. Fluid Mech. **807**, 155–166 (2016)
Liu, B., Tang, J., Huang, H., Lu, X.Y.: Deep learning methods for super-resolution reconstruction of turbulent flows. Phys. Fluids **32**, 2 (2020)
Marí Beffa, G.: Hamiltonian evolution of curves in classical affine geometries. Phys. D **238**, 100–115 (2009)
Marí Beffa, G., Olver, P.J.: Poisson structure for geometric curve flows in semi-simple homogeneous spaces. Regul. Chaotic. Dyn. **15**, 532–550 (2010)
Marí Beffa, G., Sanders, J.A., Wang, J.P.: Integrable systems in three-dimensional Riemannian geometry. J. Nonlinear Sci. **12**, 143–167 (2002)
Ricca, R.L.: Inflexional disequilibrium of magnetic flux-tubes. Fluid Dyn. Res. **36**(4–6), 319 (2005)
Rogers, J.A., Someya, T., Huang, Y.: Materials and mechanics for stretchable electronics. Science **327**, 1603–1607 (2010)
Ryu, J., et al.: Intrinsically stretchable multi-functional fiber with energy harvesting and strain sensing capability. Nano Energy **55**, 348–353 (2018)
Sarkar, J.: A critical review on convective heat transfer correlations of nanofluids. Renew. Sustain. Energy Rev. **15**(6), 3271–3277 (2011)
Sordo, F., et al.: Microstructured fibers for the production of food. Adv. Mater. **31**, e1807282 (2019)
Sun, H., Zhang, Y., Zhang, J., Sun, X., Peng, H.: Energy harvesting and storage in 1D devices. Nat. Rev. Mater. **2**, 17023 (2017)
Whitesides, G.M.: The origins and the future of microfluidics. Nature **442**(7101), 368–373 (2006)
Yan, W., et al.: Advanced multimaterial electronic and optoelectronic fibers and textiles. Adv. Mater. **31**, 1802348 (2019)